TENCON 2023 - 2023 IEEE Region 10 Conference (TENCON)
31 Oct - 3 Nov 2023. Chiang Mai, Thailand

High-frequency characteristics of photogenerated carriers in AlGaN/GaN HEMTs

Kento Kondo
Department of Electrical and Electronic Engineering, School of Engineering
Chukyo University
Nagoya, Japan
t22310m@m.chukyo-u.ac.jp

Yuki Shimizu
Department of Electrical and Electronic Engineering, School of Engineering
Chukyo University
Nagoya, Japan
t22206m@m.chukyo-u.ac.jp

Atsuya Fujiwara
Department of Electrical and Electronic Engineering, School of Engineering
Chukyo University
Nagoya, Japan
t22211m@m.chukyo-u.ac.jp

Haruki Hayashi
Department of Electrical and Electronic Engineering, School of Engineering
Chukyo University
Nagoya, Japan
t22318m@m.chukyo-u.ac.jp

Hirohisa Taguchi
Department of Electrical and Electronic Engineering, School of Engineering
Chukyo University
Nagoya, Japan
htaguchi@sist.chukyo-u.ac.jp

Abstract—**In this study, we experimentally observed the behavior of carriers generated by the photoelectric effect in the GaN crystal layer (channel layer) from the viewpoint of high-frequency characteristics to clarify the carrier transport phenomenon. It was found that the accumulation of holes generated by the photoelectric effect near the source electrode causes a new parasitic capacitance component that depends on the gate voltage.**

Keywords—AlGaN/GaN-based HEMTs, photoelectric effect, frequency dependence, hole accumulation, parasitic capacitance

I. INTRODUCTION

Digital transformation (DX) and green transformation (GX) are two major challenges in the contemporary world [1,2]. In the future, building an information and communication technology (ICT) system that pursues power-saving effects will be essential. Therefore, there is a strong demand for high-efficiency power semiconductor devices [3]. Electronic devices using GaN-based semiconductors are attractive power semiconductor devices for power-supply circuits because of their high breakdown field strength and high electron mobility caused by two-dimensional electron gas (2DEG) [4,5]. Therefore, the development of AlGaN/GaN high-electron-mobility transistors (HEMTs) is progressing rapidly toward practical applications. However, AlGaN/GaN-based HEMTs suffer from insufficient current collapse due to crystal defects in the AlGaN crystal layer [6,7], thereby limiting their use as power devices. AlGaN/GaN-based HEMTs have a unique structure that can suppress current collapse and is not found in other HEMTs [8, 9]; however, these characteristic structures also complicate the behavior of carriers in the two-dimensional electron gas formed in the channel layer. Therefore, in this study, photogenerated carriers whose generation amount could be controlled artificially were generated in a two-dimensional electron gas, and the carrier behavior in the channel layer was observed. We analyzed the behavior of the photogenerated carriers from the viewpoint of high-frequency gain and constructed a carrier behavior model in a two-dimensional electron gas. As a result ,the high-frequency characteristics of the photogenerated carriers were clarified.

II. EXPERIMENTAL METHOD

In this experiment, optical carriers were generated by irradiating the AlGaN/GaN HEMT (DUT) from above with a laser beam having an energy higher than the bandgap of the GaN crystal. Optical carriers were generated in the gaps between the gate metal and the source and drain metals. The Thorlabs epoxy-encased LED370E used in this experiment has a wavelength of 370 nm and an energy value of 3.36 eV. The output of LED370D was 1 mW/cm².The light emitted from the LED was condensed into a circle with a diameter of 25 μm by a condenser lens. The light intensity was 5.09×10^9mW.The light emitted from the light source was polarized into a parallel beam using aspheric condenser lenses and irradiated onto the DUT. Additionally, the carrier behavior inside the channel layer was observed by measuring the S-parameter frequency characteristics using a vector network analyzer. Fig. 1 shows a block diagram of the experimental system used in this study. In the high-frequency measurement, the drain voltage of the DUT was set to 1.5 V under the condition that the current collapse phenomenon occurs. The measurement frequency band ranged from 10 MHz to 10 GHz. The gate voltage was set to 0.1 V from 1.8 V to 2.4 V. For comparison purposes, the high-frequency characteristics were measured in both the ON and OFF states of the light. In the high-frequency measurement, the power gain characteristic S_{21} parameter was extracted, and the current gain characteristic h_{21} parameter was derived from the data.

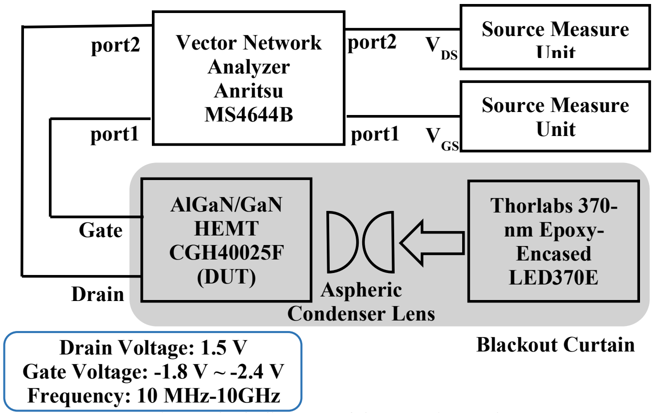

Fig.1. Block diagram of the experimental system.

979-8-3503-0219-6/23/$31.00 ©2023 IEEE

III. Results And Discussions

A. *Frequency dependence of power gain (S_{21})*

Fig. 2 shows the frequency dependence of the power gain when the DUT is not irradiated with a parallel beam. Fig. 3 shows the frequency dependence of the power gain after irradiating the DUT with a parallel beam. A comparison of Figs. 2 and 3 confirms that the parallel-beam irradiation reduces the power gain in the high-frequency band. Fig. 4 shows a schematic of the carrier behavior inside the channel layer. Electron-hole pairs were generated inside the channel layer by parallel beam irradiation. The electrons generated by the parallel beam degenerate inside the channel layer and become 2DEG, which goes through to the drain end as it is. However, although the holes move toward the source electrode, the transport stops near the source electrode because of the potential barrier created by GaN and AlGaN [10]. Therefore, holes start to accumulate near the source electrode and function as circuit factors that degrade the response performance in the high-frequency region [11].

Fig. 5 shows the gate-voltage dependence of the power-gain cutoff frequency. The orange and blue lines represent the parallel beam ON and OFF states, respectively. As the gate voltage decreases, the power-gain cutoff frequency increases. The power gain cutoff frequency for parallel beam ON is lower than that for parallel beam OFF. However, a reversal phenomenon is confirmed at a gate voltage of -2.4V. This is attributed to the number of electrons in the 2DEG. By lowering the gate voltage, the electron density in the 2DEG decreases. It is conceivable that the holes that accumulated in the vicinity of the source electrode are more localized as the 2DEG electron density is higher. The localization of holes is considered to be an apparent circuit factor. Conversely, when the electron density of the 2DEG becomes low, hole accumulation spreads over the entire channel layer, and its functionality as a circuit factor is lost.

B. *Frequency dependence of current gain (h_{21})*

Fig. 6 shows the frequency dependence of the current gain when the DUT is not irradiated with a parallel beam. Fig. 7 shows the frequency dependence of the current gain after irradiating the DUT with a parallel beam. Similar to the frequency dependence of the power gain, the gain decreased with parallel-beam irradiation. Figure 8 shows the gate voltage dependence of the current-gain cutoff frequency. The orange and blue lines represent the parallel beam ON and

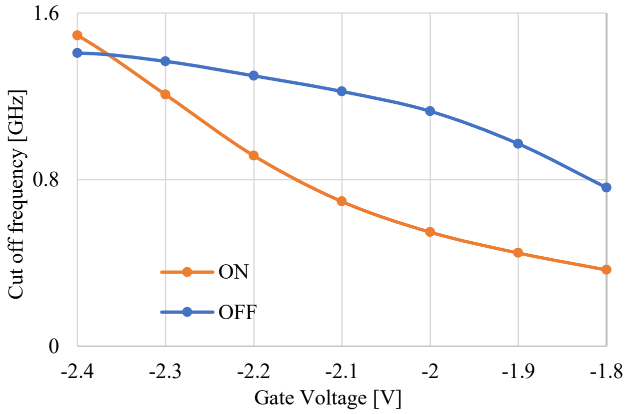

Fig. 5. Gate-voltage dependence of the power-gain cutoff frequency.

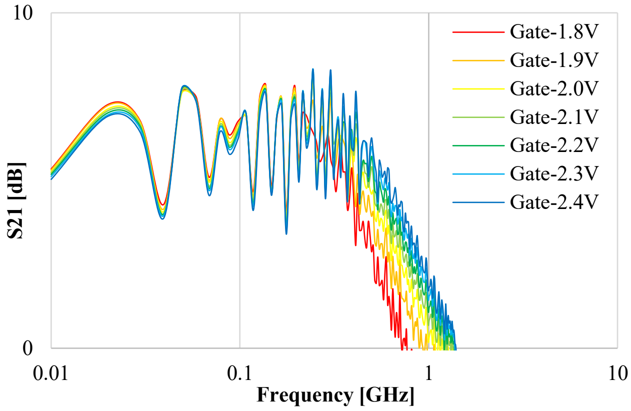

Fig. 2. Frequency dependence of the power gain. (Not irradiated with a parallel beam)

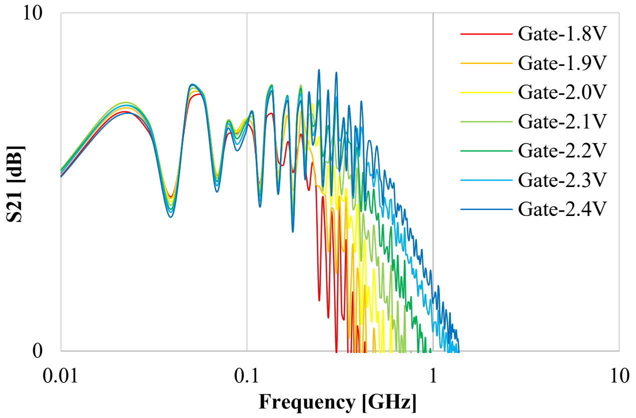

Fig. 3. Frequency dependence of the power gain. (Irradiated with a parallel beam)

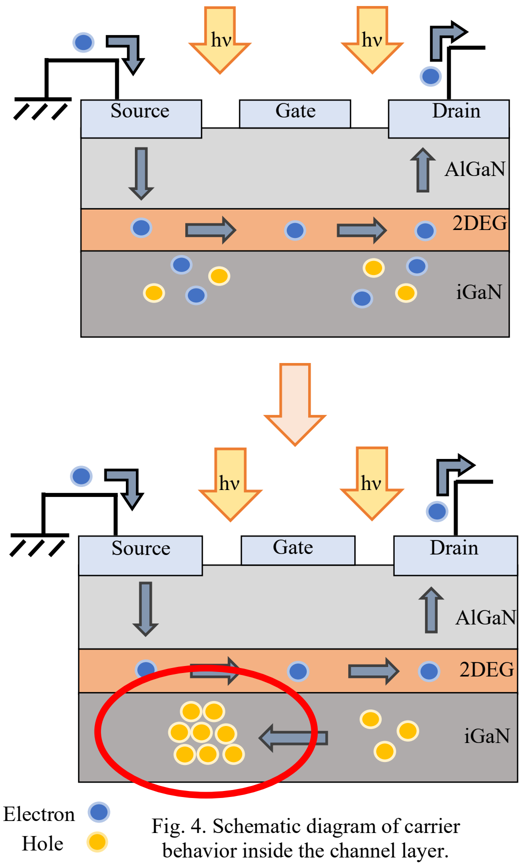

Fig. 4. Schematic diagram of carrier behavior inside the channel layer.

OFF states, respectively. The trends in Fig. 8 are almost similar to those in Fig. 5.

A crossing point can be clearly confirmed in the frequency dependence of the current gain in Figs. 6 and 7. Fig. 8 shows an enlarged view of the crossing point in Fig. 7. Normally, both the power and current gains are attenuated at a constant rate [12]. Unlike the power gain (S_{21}), the current gain (h_{21}) is a theoretical calculation obtained using a small-signal circuit model of MESFET [13]. This implies that the current gain decay deviates from the theoretical curve, which indicates that the adaptation of the small-signal circuit model is inappropriate. GaN-based HEMTs exhibit a current collapse phenomenon [14]. The current collapse phenomenon is caused by the trapping of 2DEG in the crystal defects in the AlGAN layer [15]. In other words, the occurrence of crossing points in Fig. 6 is considered to be due to crystal defect factors, regardless of the presence or absence of parallel beams. Furthermore, as confirmed in Fig. 7, the parallel-beam irradiation causes a deviation from the theoretical curve because the crossing point is even more apparent. Hole accumulation occurs near the source electrode of the channel layer because of parallel beam irradiation. Hole accumulation leads to an increase in the positive gate-source bias, which increases the gate-source capacitance (C_{gs}). Although C_{gs} exists as a parasitic capacitance in the MESFET small-signal circuit model [16], the bias effect due to crystal defects and the hole accumulation effect were not considered.

IV. CONCLUSIONS

In this study, photogenerated carriers, whose generation amount could be artificially controlled, were generated in a two-dimensional electron gas, and the carrier behavior in the channel layer was observed. We analyzed the behavior of photogenerated carriers from the viewpoint of high-frequency gain and constructed a carrier behavior model in a two-dimensional electron gas. We experimentally observed the behavior of carriers generated by the photoelectric effect in the GaN crystal layer (channel layer) from the viewpoint of high-frequency characteristics to clarify the carrier transport phenomenon. Hole accumulation leads to an increase in the positive gate-source bias, which increases the gate-source capacitance. It was found that the accumulation of holes generated by the photoelectric effect near the source electrode causes a new parasitic capacitance component that depends on the gate voltage.

ACKNOWLEDGMENT

The authors are grateful to the Chukyo University Research Found for financial assistance with this research.

REFERENCES

[1] J. Yan, W. Yang, Z. Min, and M. Yang, “Innovation strategy for green development and carbon neutralization in Guizhou—an overview,” Sustainability 2022, vol. 14, pp. 14377, November 2022.

[2] Z. Huan, “Pathways to carbon neutrality in major exporting countries: the threshold effect of digital transition,” Environ. Sci.Pollut. Res., vol. 30, pp. 7522–7542, January 2023.

[3] M. E. T. Souza Jr. and L. C. G. Freitas, “Power electronics for modern sustainable power systems: distributed generation, microgrids and smart grids—a review,” Sustainability, vol. 14, pp. 3597, March 2022.

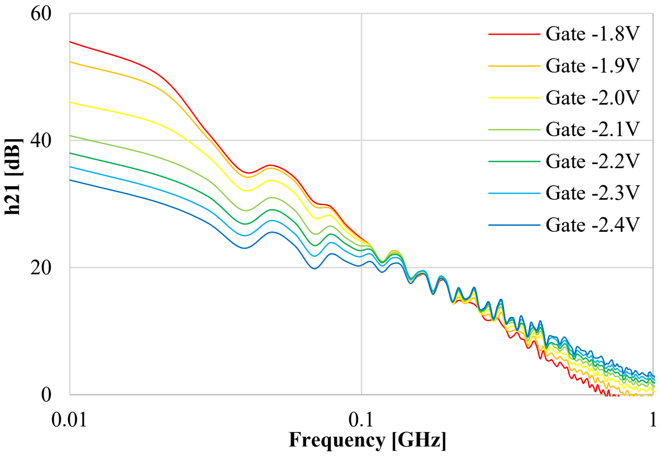

Fig. 6. Frequency dependence of the current gain. (Not irradiated with a parallel beam)

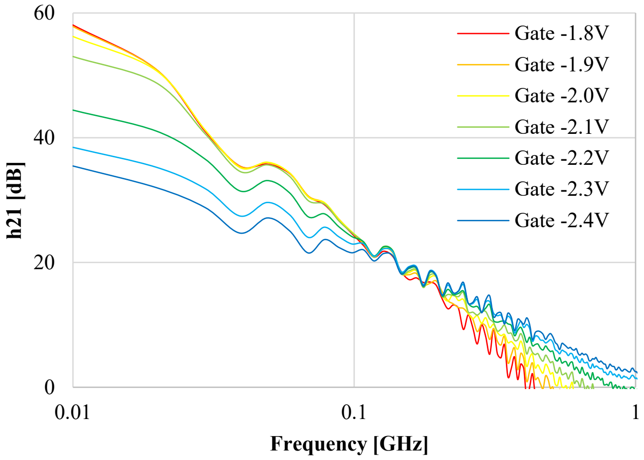

Fig.7. Frequency dependence of the current gain. (With a parallel beam)

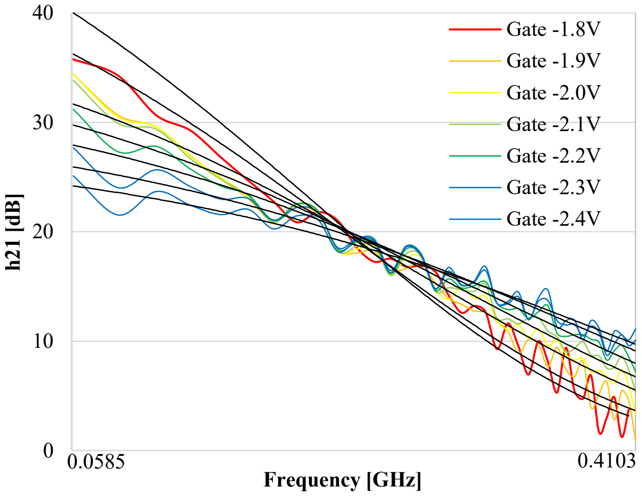

Fig. 8. Enlarged view of the crossing point in Fig.7. (Frequency range; 0.0585-0.4103 GHz)

[4] J. Millán, P. Godignon, X. Perpiñà, A. Pérez-Tomás, and J. Rebollo, "A survey of wide bandgap power semiconductor devices," IEEE Trans. Power Electron., vol. 29, pp. 2155–2163, May 2014.

[5] R. Fabrizio and L. Michael, Nitride Semiconductor Technology: Power Electronics and Optoelectronic Devices, 1st ed., John Wiley & Sons, 2020, pp. 99-127.

[6] W. Saito, T. Noda, M. Kuraguchi, Y. Takada, K. Tsuda, Y. Saito, I. Omura, and M. Yamaguchi, "Effect of buffer layer structure on drain leakage current and current collapse phenomena in high-voltage GaN-HEMTs," IEEE Trans. Electron Devices, vol. 56, pp. 1371–s1376, July 2009.

[7] P. V. Raja, M. Bouslama, S. Sarkar, K. R. Pandurang, J. Nallatamby, N. DasGupta, and A. DasGupta, "Deep-level traps in AlGaN/GaN- and AlInN/GaN-based HEMTs with different buffer doping technologies," IEEE Trans. Electron Devices, vol. 67, pp. 2304–2310, June 2020

[8] Y. Kumazaki, T. Ohki, J. Kotani, S. Ozaki, Y. Niida, K. Makiyama, Y. Minoura, N. Okamoto, N. Nakamura and K. Watanabe, "Remarkable current collapse suppression in GaN HEMTs on free-standing GaN substrates," 2019 IEEE BiCMOS and Compound Semiconductor Integrated Circuits and Technology Symposium (BCICTS), Nashville, TN, USA, 2019, pp. 1–4

[9] S. Gao, Q. Zhou, X. Liu, and H. Wang, "Breakdown enhancement and current collapse suppression in AlGaN/GaN HEMT by NiOX/SiNX and Al2O3/SiNX as gate dielectric layer and passivation layer," IEEE Electron Device Lett., vol. 40, pp. 1921–1924, December 2019.

[10] G. Koley and M. G. Spencer, “Surface potential measurements on GaN and AlGaN/GaN heterostructures by scanning Kelvin probe microscopy,” J. Appl. Phys., vol. 90, pp. 337–344, July 2001

[11] A. Stockman, E. Canato, M. Meneghini, G. Meneghesso, P. Moens, and B. Bakeroot, "Threshold voltage instability mechanisms in p-GaN gate AlGaN/GaN HEMTs," 2019 31st International Symposium on Power Semiconductor Devices and ICs (ISPSD), Shanghai, China, 2019, pp. 287-290

[12] J. C. Zolper, "A review of junction field effect transistors for high-temperature and high-power electronics," Solid State Electron., vol. 42, pp. 2153–2156, December 1998.

[13] V. Camarchia, F. Cappelluti, G. Ghione, E. Limiti, D. A. J. Moran, and M. Pirola, "An overview on recent developments in RF and microwave power H-terminated diamond MESFET technology," 2014 International Workshop on Integrated Nonlinear Microwave and Millimetre-wave Circuits (INMMiC), Leuven, Belgium, pp. 1–6, April 2014.

[14] F. Berthet, Y. Guhel, H. Gualous, B. Boudart, J. Trolet, M. Piccione, V. Sbrugnera, B. Grimber, and C. Gaquière, "Characterization and analysis of electrical trap related effects on the reliability of AlGaN/GaN HEMTs," Solid State Electron., vol. 72, pp. 15–21, March 2012.

[15] A. Y. Polyakov and I-H. Lee, "Deep traps in GaN-based structures as affecting the performance of GaN devices," Materials Science and Engineering: R: Reports, Vol. 94, pp. 1–56, August 2015.

[16] E. Rabaie, E. Sayed, "Nonlinear simulation methods for active microwave circuits: a review of the art and novel trends," Int. J. Nano Device Sens. Syst., vol. 1, pp. 77–101, October 2012.